Experimental Validation of IEEE 802.11ah Propagation Models in Heterogeneous Smart City Environments

Tobia De Koninck, Serena Santi, Jeroen Famaey, Filip Lemic
Internet Technology and Data Science Lab (IDLab), University of Antwerpen - imec, Belgium
Email: tobia.dekoninck@student.uantwerpen.be, {serena.santi, jeroen.famaey, filip.lemic}@uantwerpen.be

***Abstract*—IEEE 802.11ah is a novel sub-GHz license-free WiFi technology that is of great interest for Smart Cities, primarily due to its long range, low energy consumption, reliability, and ubiquitousness. To guarantee a long lifetime of battery-powered IEEE 802.11ah Mobile Terminals (MTs), network discovery based on beacon listening or active probing should ideally be avoided. Alternative discovery approaches heavily rely on crowd-sourcing, which in turn relies on propagation modeling. Due to the novelty of IEEE 802.11ah, the accuracy of the available propagation models is currently all but clear, and this paper makes one of the first steps in bridging this gap. Specifically, for a number of Smart City-relevant environments we experimentally evaluate the accuracy of an exhaustive set of propagation models by comparing their outputs against real measurements obtained using IEEE 802.11ah-compatible hardware. Our results are encouraging, showing that the existing models are indeed suitable for IEEE 802.11ah. However, they also indicate that diverse models perform best in distinct types of deployment environments, suggesting the need for an environment-tailored design of IEEE 802.11ah-based systems that utilized propagation modeling.**

I. INTRODUCTION

A variety of Internet of Things (IoT) use-cases require a wireless communication technology that features high coverage and low energy consumption. This is a particularly strong requirement in the context of Smart Cities that envision use-cases such as long-term and long-range tracking of objects (e.g., construction equipment, postal trucks) or environmental monitoring (e.g., pollution, hazardous gases). Low-Power Wide Area Network (LPWAN) technologies operating in the sub-GHz Short-Range Device (SDR) frequency band are among the most suitable candidates for supporting such use-cases. Among them, IEEE 802.11ah (i.e., WiFi HaLow) is expected to provide several advantageous features pertaining to a simple setup (due to the widespread deployment of IEEE 802.11), reliable communication (due to frequency, time, and space diversity), and extended lifetime (due to short data transmissions and various implemented battery saving strategies) [1], [2]. For these reasons, in the near future IEEE 802.11ah is expected to become one of the most prominent communication technologies in the Smart City context.

Due to the fact that the deployment environments are expected to be relatively large, full coverage cannot be guaranteed. In addition, the envisioned use-cases will not require continuous connectivity between the Mobile Terminals (MTs) and the core infrastructure, i.e., there will be a possibility for the data to be delivered intermittently. To guarantee a long lifetime of the battery-powered MTs, IEEE 802.11ah used for the communication between the MT and the core infrastructure should be operational only when a communication link featuring the desired data-rate can be established. A widely used metric for deciding if such a communication link can be established is the Signal-to-Noise Ratio (SNR). Moreover, the usual procedure to obtain the SNR estimate is through beacon listening or active probing, which however consume relative large amounts of energy, negatively affecting the lifetime of the MT [3], [4].

To avoid this energy dissipation, the decision if the communication between the MT and the core IEEE 802.11ah infrastructure should be initiated can be based on an Radio Environmental Map (REM), i.e., a footprint of a radio environment [5]. In such an approach, the MT is able to check the prestored SNR at its given location before deciding if the communication with the core infrastructure should be initiated, which removes the need for beacon listening or active probing. This is a feasible approach for the envisioned use-cases (e.g., asset tracking, environment monitoring) as they unavoidably require the location of the MT [3]. Given that this approach requires an REM, it is obvious that the REM has to be somehow generated. The prevalent minimum-effort approach in generating the REM is to utilize crowd-sourcing, which is particularity suitable for IEEE 802.11ah due to the omnipresence of IEEE 802.11 technology on mobile devices [1].

Crowd-sourcing generally yields a discrete set of spatially distributed measurements. In order to generate a complete REM of an environment (i.e., for all locations in an environment of interest), there is a need for estimating the SNR values at the locations not covered by measurements [6]. An established procedure for doing that is to utilize an accurate propagation model for estimating the expected SNR at non-crowd-sourced locations. However, due to the novelty of the technology and the consequent lack of hardware support, an experimental characterization of the suitability of different propagation models is currently lacking for IEEE 802.11ah. This paper makes one of the first steps in resolving this issue.

Specifically, in this paper we evaluate the suitability of several available propagation models for the IEEE 802.11ah technology. Contrary to the majority of existing works that utilize simulated and unvalidated models (e.g., [7], [8]), we characterize the feasibility of the models by comparing their outputs against real physical layer measurements obtained using IEEE 802.11ah-compatible hardware. We focus on a heterogeneous set of Smart City-relevant deployment environments (i.e., urban, suburban, and indoor), in contrast to existing efforts focusing solely on outdoor urban environments [9]. Finally, we contribute by characterizing the packet loss in the different deployment environments. This makes it possible to not only to generate an REM, but also to determine the SNR limits below which reliable communication can be established.

II. Propagation Models

This section provides a short overview of the propagation models considered in this work.

1) COST-231 Hata: This is an outdoor path loss model where the antenna of the base station is assumed to be deployed on a rooftop level [10]. The modeled path loss is given in Equation (1), with the parameters being the central frequency f [MHz], distance between the devices d [km], heights of the base station h_{base} [m] and of the MT h_{mobile} [m]. The definitions of $a(h_{mobile})$ and C_m are given in [10].

$$\begin{aligned} L_b = {} & 46.3 + 33.9\log_{10}(f) \\ & - 13.82\log_{10}(h_{base}) - a(h_{mobile}) \\ & + (44.9 - 6.55\log_{10}(h_{base}))\log_{10}(d) + C_m. \end{aligned} \tag{1}$$

2) COST-231 Walfisch-Ikegami: This model aims at improving the COST-231 model by accounting for additional parameters of an environment (i.e., height of buildings, width of roads, distance between buildings, and road orientation) [10]. It has a different definition for both Line-of-Sight (LoS) and Non-Line-of-Sight (NLoS) conditions, given by Equation (2) and Equation (3), respectively. The model defines the following parameters: central frequency f [MHz], distance between devices d [km], road width w [m], road orientation (with respect to the direct radio path) φ [°], height of the base station h_{base} [m] and MT h_{mobile} [m], and height of buildings h_{roof} [m]. The equation for NLoS depends additional parameters fully specified in [10].

$$L_b = 42.6 + 26\log_{10}(d) + 20\log(f) \text{ for } d \geq 20\,\text{m}, \tag{2}$$

$$L_b = \begin{cases} L_0 + L_{rts} + L_{msd} & \text{for } L_{rts} + L_{msd} > 0 \\ L_0 & \text{for } L_{rts} + L_{msd} \leq 0. \end{cases} \tag{3}$$

3) Ah Macro: This outdoor path model loss is defined in [8] (Equation (4)), with the sole parameter being the distance between devices d [m].

$$L_b = 8 + 37.6\log_{10}(d). \tag{4}$$

4) Ah Pico: The modeled path loss is in this model [8] given by Equation (5). The parameters are the distance between devices d [m] and operating frequency f [MHz].

$$L_b = 23.3 + 37.6\log_{10}(d) + 21\log_{10}\left(\frac{f}{900}\right). \tag{5}$$

5) Ah Indoor: This indoor model is based on the IEEE 802.11n model, but scaled down to the frequency of IEEE 802.11ah. The model accounts for the free space loss up to a certain breaking-point distance [8]. Besides the usual parameters for the distance between the devices d [m] and central frequency f [MHz], this model includes a parameter for the breaking-point distance d_{BP} [m]. The modeled path loss is defined as:

$$L_b = \begin{cases} L_{FS} & \text{for } d \leq d_{BP} \\ L_{FS} + 3.5\log_{10}\left(\frac{d}{d_{BP}}\right) & \text{for } d > d_{BP}, \end{cases} \tag{6}$$

where L_{FS} is defined as:

$$L_{FS} = 20\log_{10}\left(\frac{4\pi df}{c}\right). \tag{7}$$

6) ITU-R Below Rooftop: As specified by ITU-R [11], this model can be used in urban or residential environments when the antennas are at a low height (i.e., near the street level and well below the rooftop height). The model contains LoS and NLoS regions, while in the transition between regions the path loss decreases rapidly. After the transition region, the path loss is modeled as a linear interpolation between the LoS and NLoS path losses. In addition, the model also contains the so-called location percentage p, i.e., a parameter used for specifying the percentage of locations at which the modeled path loss is not exceeded. The full definition of the LoS and NLoS cases is given in [11].

$$L_b = \begin{cases} L_{LoS} & \text{for } d < d_{LoS} \\ L_{NLoS} & \text{for } d > d_{LoS} + w \\ LoS + (L_{NLoS} - L_{LoS}) \\ \quad \cdot (d - d_{LoS})/w & \text{otherwise} \end{cases} \tag{8}$$

III. Evaluation Scenarios

In this section, we discuss the evaluation scenarios for which our measurement campaigns have been carried out. These scenarios have been selected primarily due to their relevance in the context of the Smart Cities.

1) Scenario 1: The first scenario represents a suburban environment with mostly LoS connectivity (Figure 1(a)). It features an unpaved road with an approximate width of $6\,\text{m}$ in a forest, surrounded by buildings. The transmitting and receiving devices were positioned horizontally and facing each other. There were only minor activities during the experimentation, such as a few the cars passing by. The measurement campaign lasted roughly $45\,\text{min}$, during which in total respectively 85320 packets were sent and 48989 packets were received.

2) Scenario 2: This scenario represents an urban environment with mostly NLoS connectivity (Figure 1(b)). We have selected an urban residential neighborhood in the city of Antwerp, Belgium, partially enclosed by a forest and a waterway. There are about 350 detached houses inside the measurement area ($\approx 0.55\,\text{km}^2$). The buildings feature at most two floors. The antennas of both the receiving and transmitting modules were placed upwards. While the receiving antenna

(a) Scenario 1 (b) Scenario 2 (c) Scenario 3

Figure 1. Schematic footprints of the evaluation scenarios

TABLE I
IEEE 802.15.4G MCSS FOR OPTION 1 (SOURCE: [13])

MCS Index	Modulation	Coding rate	Frequency Repetition	Data rate (kbps)	802.11ah MCS
0	BPSK	1/2	4x	100	N/A
1	BPSK	1/2	2x	200	N/A
2	QPSK	1/2	2x	400	N/A
3	QPSK	1/2	No	800	1
4	QPSK	3/4	No	1200*	2
5	16-QAM	1/2	No	1600*	3
6	16-QAM	3/4	No	2400*	4

TABLE II
IEEE 802.11AH MCSS FOR 1, 2 MHZ, NSS = 1, GI = 8 US (SOURCE: [7])

MCS Index	Modulation	Coding rate	Data rate (kbps)	
			1 Mhz	2 Mhz
0	BPSK	1/2	300	650
1	QPSK	1/2	600	1300
2	QPSK	3/4	900	1950
3	16-QAM	1/2	1200	2600
4	16-QAM	3/4	1800	3900
5	64-QAM	2/3	2400	5200
6	64-QAM	3/4	2700	5850
7	64-QAM	5/6	3000	6500
8	256-QAM	3/4	3600	7800
9	256-QAM	5/6	4000	N/A
10	256-QAM	1/2 (2x repetitions)	150	N/A

was positioned at a fixed place inside a garden, the transmitting antenna was being moved along the roads. During the measurement campaign a number of cars, pedestrians, and bicycles passed by. This measurement campaign took roughly $2.5\,\mathrm{h}$, which resulted in a total of 341280 sent packets and 121658 received packets.

3) Scenario 3: This scenario represents an indoor environment, with mostly NLoS propagation conditions (Figure 1(c)). To create such a scenario, a university building has been selected, with a footprint of roughly $2000\,\mathrm{m}^2$. This building has three floors and mostly non-solid concrete walls. Note that there are some open spaces inside the building, e.g., around the staircases and above the main hall. The receiving module was placed at the second floor, while the transmitting one was positioned at different locations on the first, second, and third floors in the building. The measurement campaign took roughly $70\,\mathrm{min}$, during which 50694 of the 130824 sent packets were actually received. The campaign was done during the weekend and there were no people present at the premises.

IV. Measurement Methodology

To the best of our knowledge, hardware implementations of the IEEE 802.11ah technology are currently not available. Due to this constraint, as a workaround solution in our measurement campaigns we have used two OpenMote B modules originally implementing the IEEE 802.15.4g technology. We did that as the sub-GHz IEEE 802.15.4g radio included in the modules features a partial support for a subset of the modulation and coding schemes of IEEE 802.11ah [12].

Specifically, the IEEE 802.15.4g standard defines, in addition to the Modulation and Coding Schemes (MCSs), the potential use of an "option" parameter, with the possible values being 1, 2, 3, and 4. In this work, we have set the option to 1, which utilizes a bandwidth of $1\,\mathrm{MHz}$ (Table I), i.e., the minimal bandwidth in IEEE 802.11ah (Table II).

Note that in Table I the MCSs marked with "*" are not compliant with the IEEE 802.15.4g standard, although they are supported by the OpenMotes. The first three MCSs (i.e., 0, 1, 2) of IEEE 802.15.4g use frequency repetitions and are therefore incompatible with IEEE 802.11ah. Hence, the first MCS considered in this work is MCS 3 (referred to as MCS 1 in IEEE 802.11ah). In addition, MCS 5 in IEEE 802.15.4g (MCS 3 in IEEE 802.11ah) is considered.

The transmitting OpenMote B module is held by a person walking around the measurement environment. Simultaneously, the receiving module is placed on a pole at $1.5\,\mathrm{m}$ above the ground, logging the collected measurements. Both modules run a program adapted from the OpenWSN project. The transmitter module continuously transmits packets of 509 bytes with 4 additional bytes for the Cyclic Redundancy Check (CRC). During an interval of 5 seconds the transmitter sends 158 packets, with the resulting throughput of $129\,\mathrm{kbps}$. This is lower than the maximum PHY-layer data rate supported by MCS 1 and 3 in, as shown in Table II, as not to overload the devices. When the second module receives a packet, this message is logged to a computer over a serial interface. Each message contains the length of the packet, packet number, timestamp, SNR, and the indication of the CRC correctness.

For the outdoor scenarios (Scenarios 1 and 2), a smartphone navigation application was used to continually log the current time, as well as the Global Positioning System (GPS)-originating location of the transmitting module. The timestamps on the transmit and receive sides were then correlated for mapping of the received packets and the transmitting locations. As the GPS measurements feature relatively large errors for indoor environments (i.e., an average error of around $30\,\mathrm{m}$ was observed in our measurement campaigns), we have utilized an alternative approach for correlating received packets and transmitting locations in Scenario 3. Specifically, the locations of the measurement points were labeled on the floor of the building, after which the distance of each point to the receiving module was established using a highly accurate laser-base distance measuring device. By utilizing this approach, virtually exact transmitting locations and distances between modules were known for all packets.

The transmission power was configured to the maximal supported value by the radio chip, i.e. $14.5\,\mathrm{dBm}$, for all experiments and scenarios. Both OpenMote B modules utilized Atmel AT86RF215 transceivers that report Received Signal Strength Indication (RSSI) as a signed integer between -127 and 4. The -127 value indicates an invalid RSSI value, which never occurred during the tests. In addition, the transceivers reported the measured noise-floor, which was, in combination with the observed RSSI values, used for determining the SNR.

V. Evaluation Methodology and Results

We used a cost function for the evaluation of the suitability of different propagation models for IEEE 802.11ah. Moreover, we used Mean Absolute Error (MAE) in this function, instead of the more often utilized Root Mean Square Error (RMSE), as it is less sensitive to outliers. This is a desirable property in our evaluation because the propagation models should be fairly generic, hence the used metric should not be prone to the outliers in the measurements. Finally, the packet loss was calculated in the processing phase simply as a ratio between the number of received and transmitted packets. Only the packets with the correct CRC were considered as the received ones. Figure 2 depicts the modeled path losses vs. measured values for all evaluation scenarios and different MCSs. Furthermore, MAEs for different scenarios are summarized in Table III. The measured path loss is directly based on the SNR and the used transmission power. In Scenario 1 and for both considered MCSs the signal is able to propagate at most $186\,\mathrm{m}$ further than in Scenario 2. Similarly, in Scenario 2 the obtainable range is roughly an order of magnitude higher than in Scenario 3. These observations are intuitive, as that there are less obstacles attenuating the signals in Scenario 1 (sub-urban environment) than in Scenario 2 (urban environment), and less obstacles and consequently less attenuation in Scenario 2 than in Scenario 3 (indoor environment).

Moreover, as visible from the figure and the table, for both MCSs the optimal propagation model in Scenario 1 is the "Ah Pico". Moreover, in Scenario 2 the optimal model for both MCSs is the "COST-231 Hata", as visible in Figure 2 and Table III. It is also worth noting that the "ITU-R Below Rooftop" achieves comparable results, with the difference between MAEs of the two models being around 7% for both MCSs. In contrast, the best performing model in Scenario 1 ("Ah Pico") is only the third best performing model in Scenario 2, with more than 20% lower accuracy than the "COST-231 Hata" and the "ITU-R Below Rooftop". In Scenario 3, the best preforming is the "COST-231 Walfisch-Ikegami" model. This is consistent across different floors of the building, as well as for both MCSs. It is interesting to observe that this is one of the worst performing models in Scenario 1.

The above observations indicate that the existing models provide high accuracy in modeling the IEEE 802.11ah propagation, particularly in outdoor environments. This is demonstrated by relatively small MAEs of around 2 and 3 dB in Scenario 1 and Scenario 2. To put this into perspective, the average fluctuations in SNR caused by interference from nearby devices in IEEE 802.11b/g and IEEE 802.15.4 are in the range of 3 to 4 dB [14]. However, our observations also indicate that the selection of the propagation model in IEEE 802.11ah will be highly dependent on a deployment environment. Hence, the deployment environment is an important parameter to be considered in the design of IEEE 802.11ah-based systems that make use of propagation modeling.

It is also worth noting that in an indoor environment (i.e., Scenario 3) the propagation models tend to be overly optimistic, which can be judged by their consistently lower modeled path losses than the one indicated by the measurements. This is an important observation for indoor deployments of IEEE 802.11ah systems that make use of propagation modeling, which has not been made in the related research efforts (i.e., [9]). The observation indicates that, in indoor deployments, an additional attenuation parameter should be attributed to the path loss modeled using the off-the-shelf propagation models. This should be done in order to avoid their consistent underestimation of the signal attenuation. An exact characterization of the additional attenuation parameter is left for the future work.

The packet loss for different evaluation scenarios and MCSs is given in Figure 3. Moreover, Table IV provides the distances at which a given packet loss is observed in different scenarios and multiple packet loss values. For example, the row labeled with "Max d PL = 0%" in the table indicates the maximum distance at which 0% packet loss was observed.

Similar to the achievable range, it can be observed from both Figure 3 and Table IV that the packet loss increases with the distance between the modules more rapidly in Scenario 2 compared to Scenario 1, as well as in Scenario 3 compared to Scenario 2. Same as before, this is an intuitive observation occurring due to the fact that the strongest signal attenuation is expected in Scenario 3, while the weakest one is occurring in Scenario 1. In addition, the figure shows that the packet loss starts increasing roughly at the distance between devices equaling half of the achievable range for MCS 1, while this

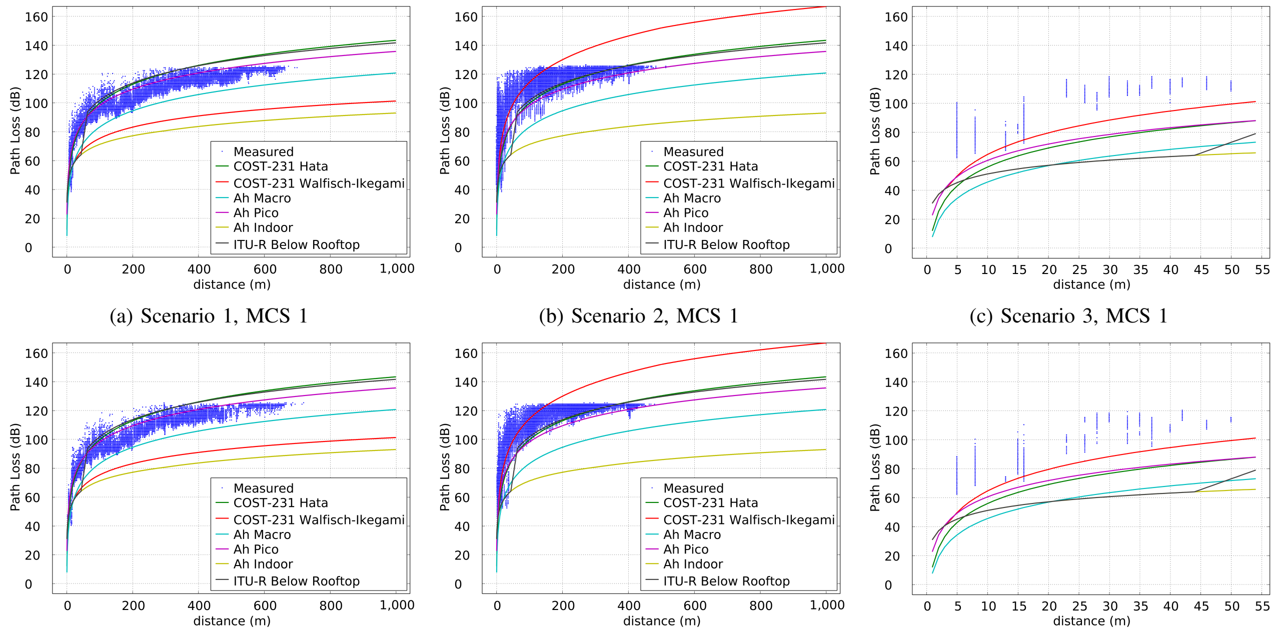

(a) Scenario 1, MCS 1 (b) Scenario 2, MCS 1 (c) Scenario 3, MCS 1

(d) Scenario 1, MCS 3 (e) Scenario 2, MCS 3 (f) Scenario 3, MCS 3

Figure 2. Comparison of measured and modeled values for different evaluation scenarios and MCSs

TABLE III
MEAN ABSOLUTE ERRORS (MAE) FOR IN DIFFERENT EVALUATION SCENARIOS

	Scenario 1		**Scenario 2**		**Scenario 3**					
	MCS 1	MCS 3	MCS 1	MCS 3	MCS 1			MCS 3		
					Floor 1	Floor 2	Floor 3	Floor 1	Floor 2	Floor 3
COST-231 Hata	4.282	3.964	**2.695**	**3.174**	8.057	7.437	6.072	8.027	8.365	5.276
COST-231 Walfisch-Ikegami	12.176	10.87	5.859	5.673	**4.864**	**4.191**	**3.692**	**4.835**	**5.118**	**3.087**
Ah Macro	5.838	5.249	9.409	10.398	11.747	11.183	8.793	11.718	12.111	7.775
Ah Pico	**2.174**	**2.060**	3.352	3.948	7.392	6.828	5.799	7.363	7.756	5.054
Ah Indoor	15.458	13.879	15.981	17.305	12.037	11.633	9.521	12.008	12.560	8.509
ITU-R Below Rooftop	4.801	4.490	2.921	3.510	11.847	11.561	9.306	11.817	12.489	8.294

increase is more rapid for MCS 3 (Table IV). These observations are consistent across different types of environments and yield a set of guidelines for the design of IEEE 802.11ah-based systems that make use of propagation modeling, which are novel contributions compared to the previous research (the most relevant one being [9]). First, in order to minimize the energy consumption, IEEE 802.11ah systems should be conservative when making propagation modeling-based decisions, especially for the lower SNR values (i.e., for larger distances between devices). This is because, even if nominally the communication link could be established, the packet losses would be considerably high for distances between the devices larger than approximately half of the achievable range. The significance of this behavior seems to be substantially more pronounced for higher MCSs, as indicated in Figure 3 and Table IV. Therefore, it seems imperative to use low MCS values if the aim is highly reliable communication, especially in indoor and urban environments. This indication is to be further evaluated as a part of our future work.

VI. CONCLUSION

In this paper, we evaluated the suitability of an exhaustive set of existing off-the-shelf propagation models for the novel IEEE 802.11ah technology. We have done that because an accurate propagation modeling will be one of the supporting pillars of many IEEE 802.11ah-based systems in the context of Smart Cities, for example the ones utilizing crowd-sourcing or fingerprinting-based localization [15]. Our evaluation was performed experimentally for heterogeneous types of environments relevant for Smart Cities, as well as for multiple IEEE 802.11ah-specific parameters. Our results yield that indeed the current propagation models are highly accurate for IEEE 802.11ah. However, their accuracy is environment-dependent, suggesting that the deployments of IEEE 802.11ah-based systems that make use of propagation modeling should be tailored for specific deployment environments. For instance, this is the case for systems using crowd-sourced information to generate a REM which is used to decide if communication with the core infrastructure is possible. This makes it possible to create intelligent handover mechanisms which avoid energy dissipation. Moreover, we have shown that a fully reliable communication can be guaranteed only for distances roughly two times lower than the attainable communication range. Future work will focus on further evaluating the derived indications, in particular for other types of environments and additional system parameters.

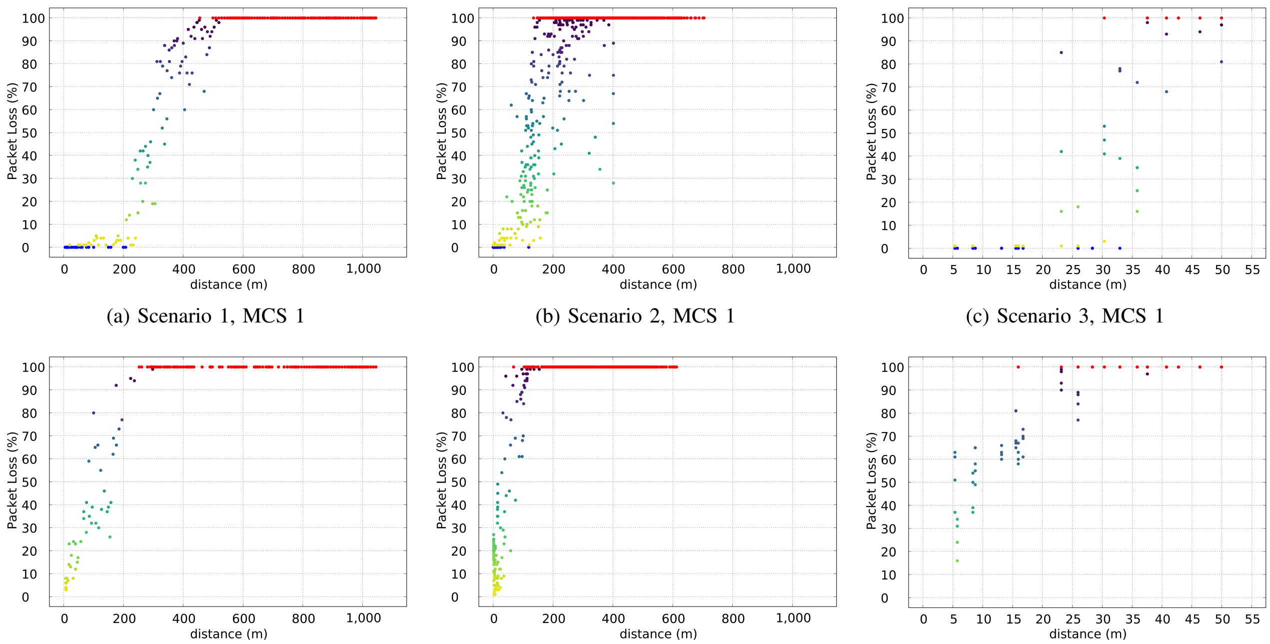

(a) Scenario 1, MCS 1 (b) Scenario 2, MCS 1 (c) Scenario 3, MCS 1

(d) Scenario 1, MCS 3 (e) Scenario 2, MCS 3 (f) Scenario 3, MCS 3

Figure 3. Packet losses for different evaluation scenarios and MCSs

TABLE IV
PACKET LOSS COMPARISON OF ALL SCENARIOS AND MCSS

	Scenario 1		**Scenario 2**		**Scenario 3**					
	MCS 1	MCS 3	MCS 1	MCS 3	MCS 1			MCS 3		
					Floor 1	Floor 2	Floor 3	Floor 1	Floor 2	Floor 3
Max d PL $= 0\%$	208 m	N/A	120 m	N/A	33 m	33 m	N/A	N/A	N/A	N/A
Max d PL $\leq 10\%$	241 m	32 m	159 m	37 m	33 m	37 m	N/A	N/A	16 m	N/A
Max d PL $\leq 20\%$	307 m	48 m	182 m	59 m	36 m	48 m	N/A	6 m	24 m	N/A

ACKNOWLEDGMENTS

This work was supported by the EU Marie Skłodowska-Curie Actions Individual Fellowships (MSCA-IF) project Scalable Localization-enabled In-body Terahertz Nanonetwork (SCaLeITN). This research was also funded by the Flemish FWO SBO S004017N IDEAL-IoT (Intelligent DEnse And Long range IoT networks) project. The author Serena Santi is funded by the Flemish FWO under grant number 1S82120N.

REFERENCES

[1] S. Aust *et al.*, "IEEE 802.11ah: Advantages in standards and further challenges for sub 1 GHz Wi-Fi," in *2012 IEEE International Conference on Communications (ICC)*, 2012, pp. 6885–6889.

[2] A. Šljivo *et al.*, "Performance Evaluation of IEEE 802.11ah Networks With High-Throughput Bidirectional Traffic," *Sensors*, vol. 18, no. 2, p. 325, 2018.

[3] F. Lemic *et al.*, "Location-Based Discovery and Vertical Handover in Heterogeneous Low-Power Wide-Area Networks," *IEEE Internet of Things Journal*, vol. 6, no. 6, pp. 10 150–10 165, 2019.

[4] S. Santi *et al.*, "On the Feasibility of Location-based Discovery and Vertical Handover in IEEE 802.11 ah," in *Wireless Communications and Networking Conference (WCNC)*, IEEE, 2020.

[5] F. Lemic *et al.*, "Enriched Training Database for Improving the WiFi RSSI-based indoor fingerprinting performance," in *Consumer Communications & Networking Conference*, IEEE, 2016, pp. 875–881.

[6] G. Caso *et al.*, "ViFi: Virtual fingerprinting WiFi-based indoor positioning via multi-wall multi-floor propagation model," *IEEE Transactions on Mobile Computing*, 2019.

[7] L. Tian *et al.*, "Extension of the IEEE 802.11ah ns-3 Simulation Module," in *Workshop on ns-3*, ser. WNS3 '18, ACM, 2018.

[8] A. Hazmi *et al.*, "Feasibility study of IEEE 802.11ah radio technology for IoT and M2M use cases," in *2012 IEEE Global Communications Conference (GLOBECOM)*, 2012, pp. 1687–1692.

[9] B. Bellekens *et al.*, "Outdoor IEEE 802.11ah Range Characterization Using Validated Propagation Models," in *2017 IEEE Global Communications Conference (GLOBECOM)*, 2017, pp. 1–6.

[10] COST Action 231 and European Commission and DGXIII Telecommunications, and Exploitation of Research, *Digital mobile radio towards future generation systems*. European Commission, 1999.

[11] *Recommendation ITU-R P.1411-10 Propagation data and prediction methods for the planning of short-range outdoor radiocommunication systems and radio local area networks*, 2019.

[12] X. Vilajosana *et al.*, "OpenMote: Open-source prototyping platform for the industrial IoT," in *International Conference on Ad-Hoc Networks*, Springer, 2015, pp. 211–222.

[13] J. Muñoz *et al.*, "Overview of IEEE 802.15.4g OFDM and its Applicability to Smart Building Applications," in *2018 Wireless Days (WD)*, IEEE, 2018, pp. 123–130.

[14] A. Behboodi *et al.*, "Interference Effect on Localization Solutions: Signal Feature Perspective," in *Vehicular Technology Conference (VTC Spring)*, IEEE, 2015, pp. 1–7.

[15] ——, "Hypothesis testing based model for fingerprinting localization algorithms," in *IEEE Vehicular Technology Conference (VTC Spring)*, IEEE, 2017, pp. 1–6.